DrivAerStar: An Industrial-Grade CFD Dataset for Vehicle Aerodynamic Optimization

Jiyan Qiu [1]
jiyanq0430@gmail.com

Lyulin Kuang [1]
lkuang@nvidia.com

Guan Wang [2]
wangguan.nantes@gmail.com

Yichen Xu [1,3,4,5]
xuyc@stu.pku.edu.cn

Leiyao Cui [3,4,5]
cuileiyaony@gmail.com

Shaotong Fu [1]
shaotongf@nvidia.com

Yixin Zhu [3,4,5,6]✉
yixin.zhu@pku.edu.cn

Ruihua Zhang [1,]✉
ritaz@nvidia.com

✉ Corresponding authors [1] NVIDIA [2] Baidu, INC. [3] Peking University
[4] State Key Lab of General AI, Peking University
[5] Beijing Key Laboratory of Behavior and Mental Health, Peking University
[6] Embodied Intelligence Lab, PKU-Wuhan Institute for Artificial Intelligence

https://drivaerstar.github.io/

Abstract

Vehicle aerodynamics optimization has become critical for automotive electrification, where drag reduction directly determines electric vehicle range and energy efficiency. Traditional approaches face an intractable trade-off: computationally expensive Computational Fluid Dynamics (CFD) simulations requiring weeks per design iteration, or simplified models that sacrifice production-grade accuracy. While machine learning offers transformative potential, existing datasets exhibit fundamental limitations—inadequate mesh resolution, missing vehicle components, and validation errors exceeding 5%—preventing deployment in industrial workflows. We present DrivAerStar, comprising 12,000 industrial-grade automotive CFD simulations generated using STAR-CCM+® software. The dataset systematically explores three vehicle configurations through 20 Computer Aided Design (CAD) parameters via Free Form Deformation (FFD) algorithms, including complete engine compartments and cooling systems with realistic internal airflow. DrivAerStar achieves wind tunnel validation accuracy below 1.04%—a five-fold improvement over existing datasets—through refined mesh strategies with strict wall y^+ control. Benchmarks demonstrate that models trained on this data achieve production-ready accuracy while reducing computational costs from weeks to minutes. This represents the first dataset bridging academic machine learning research and industrial CFD practice, establishing a new standard for data-driven aerodynamic optimization in automotive development. Beyond automotive applications, DrivAerStar demonstrates a paradigm for integrating high-fidelity physics simulations with Artificial Intelligence (AI) across engineering disciplines where computational constraints currently limit innovation.

1 Introduction

Aerodynamic optimization has become increasingly crucial as the automotive industry undergoes rapid transformation toward environmentalization, electrification, and intelligentization (Bibra et al., 2022). Precise aerodynamic design directly impacts electric vehicle range (Huluka and Kim, 2019), fuel efficiency (Abinesh and Arunkumar, 2014), fluid-excited noise (Wang et al., 2013), and high-speed stability (Brandt et al., 2022). Beyond industrial applications, high-fidelity external flow field data enables deeper integration between CFD and data-driven methods for studying complex flow

39th Conference on Neural Information Processing Systems (NeurIPS 2025) Track on Datasets and Bench-

 https://doi.org/10.52202/085713-3293

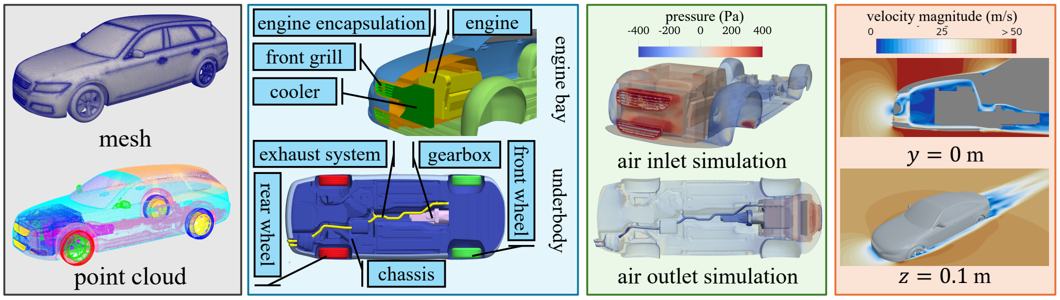

(a) geometry data formats (b) detailed components (c) fluid domain simulation (d) velocity slice

Figure 1: `DrivAerStar` **dataset features.** (a) Multiple geometry data formats: mesh (top) serves as primary representation while point cloud (bottom) enables alternative computational approaches and geometry analysis. (b) Complete vehicle modeling includes detailed engine bay compartment assembly (top) and underbody components (bottom), distinguishing `DrivAerStar` from previous automotive datasets. (c) Internal airflow simulation capabilities featuring air inlet (top) and outlet (bottom) simulations, enabled by precise internal component modeling to support comprehensive automotive system research. (d) Velocity field cross-sections showing internal engine compartment flow at vehicle centerline ($y = 0$ m) and external flow field at tire axle plane ($z = 0.1$ m).

dynamics. However, traditional numerical simulations require prohibitive computational resources, while existing datasets lack engineering fidelity for Internal Combustion Vehicle (ICV) (Payri et al., 2015), Hybrid Electric Vehicle (HEV) (Hannan et al., 2014), and Battery Electric Vehicle (BEV) (Upadhyaya and Mahanta, 2023; Bjerkan et al., 2016) applications, creating urgent demand for datasets combining precision with comprehensive parameter coverage.

Recent automotive datasets like DrivAerNet++ (Elrefaie et al., 2024) and DrivAerML (Ashton et al., 2024c) provide valuable foundations but exhibit critical limitations preventing industrial adoption. Their mesh strategies inadequately resolve gradient-dependent fields, causing boundary layer distortion and numerical diffusion errors. These resources focus on limited vehicle model deformations, failing to represent aerodynamic characteristics across diverse vehicle types and operating conditions. Furthermore, they deviate from industrial standards in turbulence modeling and solver configuration, producing results that diverge significantly from wind tunnel measurements. These shortcomings prevent the development of industrial-grade surrogate models capable of optimizing design features within minutes rather than weeks.

We present `DrivAerStar`, addressing these limitations through industrial-grade STAR-CCM+® simulations. Our approach overcomes OpenFOAM®'s inherent wall shear stress calculation deficiencies by implementing refined mesh strategies with targeted aerodynamic sensitivity refinements, sub-regional surface adaptation, and optimized boundary layer resolution. Strict control of dimensionless wall distance y^+ values (Schlichting and Kestin, 1961) ensures accurate boundary layer simulation while achieving superior computational precision with comparable mesh counts. The dataset spans multiple vehicle platforms with systematic FFD-based geometric parameter variations, representing diverse aerodynamic characteristics across vehicle types and operating conditions. Critically, we include complete front compartment assemblies with engine components and cooling systems, featuring realistic airflow channels that capture real-world vehicle aerodynamics.

Our 1,080,000 CPU core-hour computational investment across 100 nodes (see Section C.5) produces a 20 TB dataset containing 12,000 samples—50% more than existing automotive datasets. The comprehensive data covers pressure distributions, velocity vectors, turbulent kinetic energy, and high-precision aerodynamic coefficients with drag coefficient accuracy of ± 0.012. Following Loughborough University Wind Tunnel Lab specifications (Varney et al., 2020) and automobile manufacturer simulation standards, we achieve pressure coefficient errors below 1.04% compared to experimental data. Table 1 presents detailed comparisons with existing automotive CFD datasets.

To validate effectiveness, we benchmark multiple machine learning architectures, including Transolver (Wu et al., 2024), GNOT (Hao et al., 2023), and PointNet (Qi et al., 2017). Our evaluation analyzes surface pressure distributions and derived aerodynamic coefficients through surface pressure integration, establishing a multi-scale assessment for complete aerodynamic performance characterization. These benchmarks demonstrate `DrivAerStar`'s utility for training industrial-grade surrogate models while providing foundations for optimization research.

Our contributions are:

- **High-fidelity dataset**: `DrivAerStar` provides 20 TB of external flow field data from 12,000 industrial-grade STAR-CCM+® simulations across multiple vehicle configurations, delivering unprecedented data quality for surrogate model training.
- **Adaptive mesh methodology**: We employed refined mesh strategies with adaptive regional refinement and strict wall y^+ control, achieving superior boundary layer resolution that overcomes limitations of previous approaches.
- **Complete vehicle modeling**: Integration of front compartment assemblies with engines and cooling components creates continuous cooling flow channels, accurately representing real-world vehicle operating conditions.
- **Comprehensive benchmark**: We established multi-scale performance evaluation across surface and volumetric data, revealing current limitations and identifying research directions including scientific function discovery (Tang et al., 2023), forward Partial Differential Equation (PDE) problems (Lu et al., 2021; Raissi et al., 2019), simulation super-resolution (Kochkov et al., 2021), and inverse PDE reconstruction (Gao et al., 2021).

2 Related Work

Machine Learning CFD Benchmarks Large-scale, high-fidelity datasets form the foundation for deep learning applications in CFD. Recent standardized benchmarks support research in physical simulation and PDE modeling, including BubbleML (Hassan et al., 2023) for multiphase flows, Lagrangebench (Toshev et al., 2023) for Lagrangian particle-based simulations, BLASTNet (Chung et al., 2022) and BLASTNet 2.0 (Chung et al., 2023) for turbulent flow datasets, and PDEBench (Takamoto et al., 2022) for comprehensive PDE-based physical systems. While these datasets provide valuable contributions, they predominantly feature simplified geometries and idealized conditions that fail to capture the complex geometries and multiphysics interactions encountered in industrial applications.

Aerospace Aerodynamics Datasets Aerospace applications have driven advances in parameterized aerodynamic optimization through datasets enabling efficient simulation of complex geometries. AirfRANS (Bonnet et al., 2022) provides a 2D airfoil database built using OpenFOAM® with parametric meshing strategies for systematic NACA airfoil studies across operational ranges (Mach numbers 0.2–0.8, angles of attack from -8° to 20°), establishing clear mappings between geometric deformations and aerodynamic performance while providing insights into transonic shock effects. Extending to three dimensions, AircraftVerse (Cobb et al., 2023) offers 27,714 complete aircraft configurations with varied wing parameters, powertrain characteristics, and performance metrics, combining deep learning for geometry generation with engineering models for aerodynamic calculations. However, these aerospace datasets address fundamentally different flow regimes and geometric complexities than automotive applications, limiting their direct applicability to ground vehicle aerodynamics.

Automotive Aerodynamics Datasets Early automotive datasets based on simplified geometries—ShapeNet Car (Umetani and Bickel, 2018; Song et al., 2023), WindSor Car (Ashton et al., 2024a),

Table 1: **Comparative analysis of state-of-the-art automotive CFD datasets.** Quantitative benchmarking across experimental validation capabilities, numerical resolution parameters, and simulation accuracy metrics. PIV indicates flow field validation availability; wall y^+ represents dimensionless wall distance for boundary layer resolution quality; average C_D precision measures uncertainty bounds of drag coefficients; wind tunnel error shows percentage deviation from experimental measurements. Data are sourced from original literature and publicly released datasets, with detailed information available in Section E.

Metric	DrivAerNet++ (Elrefaie et al., 2024)	DrivAerML (Ashton et al., 2024c)	`DrivAerStar`
PIV	No	No	**Yes**
Engine compartment	No	No	**Yes**
Cooler	No	No	**Yes**
Samples	8,000	500	**12,000**
Wall y^+ range	$[50, 300]$	-	$[\mathbf{30}, \mathbf{200}]$
Average C_D precision	0.012	0.010	**0.005**
Wind tunnel error (%)	$\leqslant$**5.0**	$\leqslant$6.5	**1.04**

https://doi.org/10.52202/085713-3293

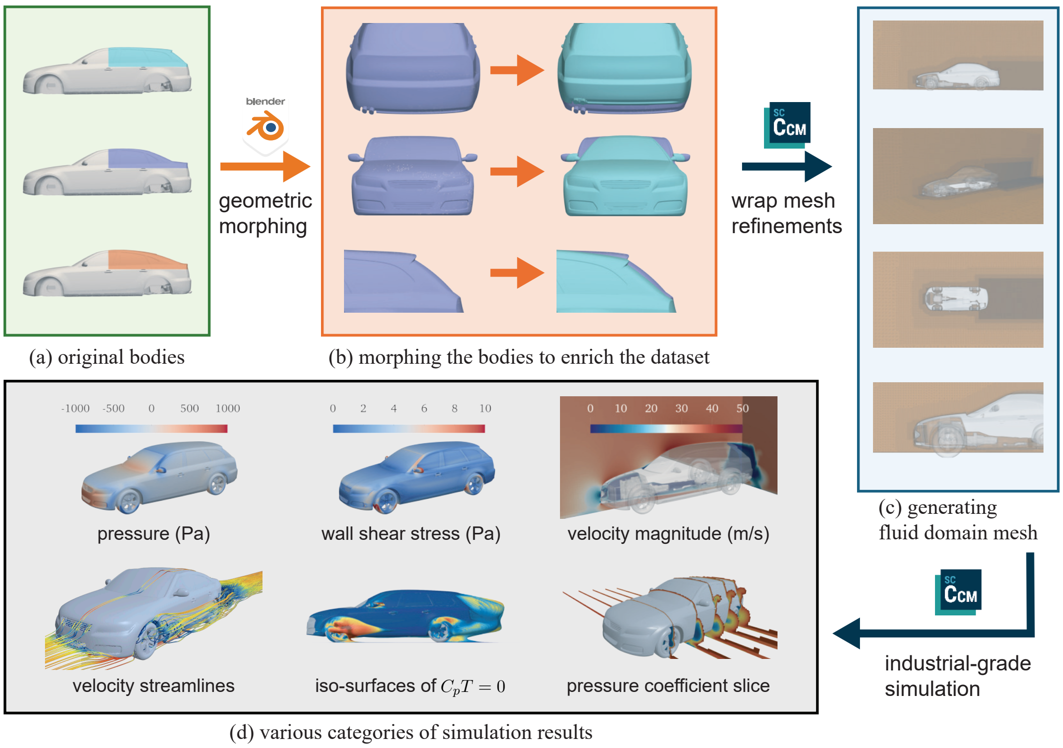

Figure 2: DrivAerStar **data generation.** (a) Three canonical DrivAer reference bodies (Estateback, Notchback, and Fastback) serve as geometric foundations. (b) Parametric morphing systematically varies 20 vehicle components, including greenhouse (top), rear diffuser (middle), and trunk lid (bottom). (c) Industrial-grade mesh generation in STAR-CCM+® produces refined hexahedral-dominant meshes with precise wheel alignment and boundary layer resolution for complex flow capture. (d) Comprehensive CFD simulations generate diverse flow visualizations: surface pressure, wall shear stress, velocity magnitude, streamline patterns, flow separation regions ($C_P = 0$ iso-surfaces), and pressure coefficient slices revealing key aerodynamic structures.

and Ahmed-body configurations (Li et al., 2023; Ashton et al., 2024b)—advanced the field but created substantial gaps between research outcomes and industrial requirements. More sophisticated approaches emerged with the DrivAerNet series, including DrivAerNet (Elrefaie et al., 2025) and DrivAerNet++ (Elrefaie et al., 2024), implementing parametric simulations using OpenFOAM®. DrivAerML similarly offers 500 parametrically morphed variants of the DrivAer Notchback model with pressure, velocity, and turbulence fields. Concurrent work by Warner and Emory (2025) introduced AeroSUV, featuring 1,000 detached eddy simulation configurations from an open-access reference model extending the DrivAer platform, executed using proprietary in-house solvers. Despite these advancements, existing automotive datasets exhibit critical limitations preventing industrial adoption: insufficient mesh resolution for complex geometries, inadequate turbulence modeling within the OpenFOAM® framework, and failure to account for crucial interactions between engine compartment thermal management and external aerodynamics.

DrivAerStar addresses these fundamental limitations by employing DrivAer vehicle geometry with the industry gold standard STAR-CCM+® solver for mesh generation and flow solution. As detailed in Table 1, our approach delivers substantial advantages in mesh resolution, aerodynamic accuracy, parametric dimensionality, and engine compartment simulation fidelity. These advancements establish a new benchmark for data-driven automotive aerodynamics research, bridging the gap between academic machine learning exploration and practical engineering applications while supporting development of general pretrained aerodynamics operator networks with potential long-term impacts detailed in Section B.

3 The DrivAerStar Dataset

Developed using industry-standard STAR-CCM+®, DrivAerStar bridges academic research and industrial applications through rigorous validation, achieving 1.04% mean relative error compared to wind tunnel measurements (Table 2). The dataset comprises 12,000 high-fidelity simulations of engine-integrated vehicle geometries, each containing STL representations with at least 4 million triangles and complementary data formats capturing surface distributions, full-field flow, and cross-sectional aerodynamic data. Our workflow (Figure 2) encompasses geometric morphing (Section 3.1), mesh generation (Section 3.2), and industrial-grade simulation (Section 3.3).

Unlike existing automotive CFD datasets, `DrivAerStar` incorporates the highest-fidelity geometric data with three rear body configurations, each featuring complete air intake, engine compartment, and cooling systems (Figure 1). To ensure industrial relevance, we systematically varied 20 fine-tuned CAD parameters (Table A1) covering both local and global vehicle features using Blender® through Latin Hypercube Sampling (LHS), creating a comprehensive design exploration space (Figure A2). The dataset spans Reynolds numbers from 9.46×10^6 to 1.48×10^7, with flow features available in volumetric, slice, and surface formats including velocity, pressure, surface properties, wall shear stress, mesh configurations, y^+ values, 3D streamlines, and iso-surfaces.

`DrivAerStar` provides comprehensive aerodynamic metrics aligned with physics field data: pressure coefficient (C_P), friction coefficient (C_F), drag coefficient (C_D), and lift coefficient (C_L). Beyond performance metrics, we supply complete numerical data (pressure, velocity, wall shear stress) alongside reproducible workflows with validation scripts following industrial standards. Simulation results are detailed in Section C.6. The dataset subset, encompassing over 12,000 VTK surface files and EnSight flow field files totaling approximately 20 TB, is accessible via our project homepage under the Creative Commons Attribution-NonCommercial-ShareAlike 4.0 International (CC BY-NC-SA 4.0) license, with data processing and benchmarking code included. Detailed licensing information is provided in Section A.

3.1 Geometric Morphing

`DrivAerStar` builds upon the experimentally validated `DrivAer` reference vehicle platform (Heft et al., 2012; Strangfeld et al., 2013), featuring three canonical rear configurations: Fastback, Estateback, and Notchback. To generate our comprehensive dataset of 12,000 geometrically diverse vehicle models, we implemented systematic FFD techniques targeting critical aerodynamic components. This approach (Figure 3) enables precise parametric control over vehicle geometry, transforming the base Fastback model into varied body and wheel configurations through controlled parameter adjustments. Complete technical details of our FFD implementation are provided in Section C.1.

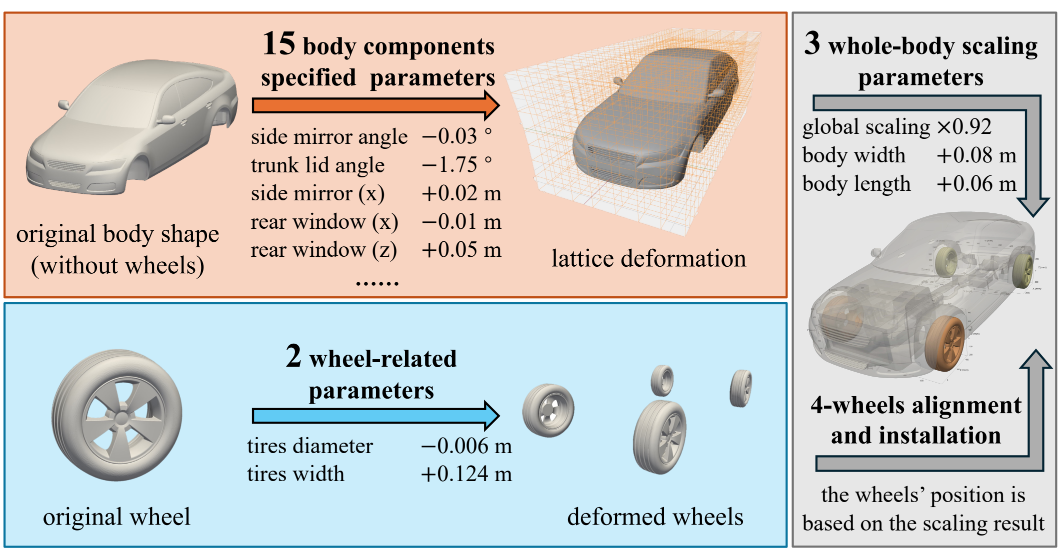

Figure 3: **Geometric morphing pipeline example.** Our parametric deformation framework transforms the baseline model through three sequential operations: (i) **Body component morphing** (top-left) applies 15 controlled parameter adjustments, including dimensional modifications and component repositioning; (ii) **Wheel morphing** (bottom-left) enables precise tire parameter control; and (iii) **Whole-body scaling and wheel installation** (right) applies 3 scaling parameters while aligning wheels to scaled positions. This systematic FFD approach generates geometrically diverse yet aerodynamically realistic vehicle configurations.

https://doi.org/10.52202/085713-3293

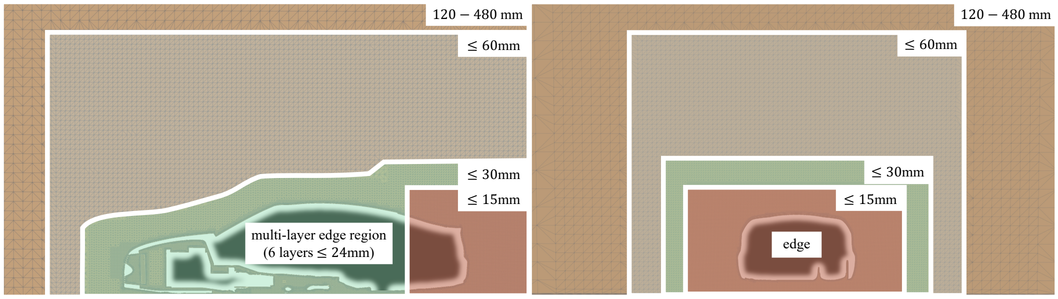

(a) mesh slice at $y = 0$ m (b) mesh slice at $x = 3.12$ m

Figure 4: **Cross-sectional views of mesh generation strategy.** (a) Longitudinal section at $y = 0$ m shows four nested refinement zones with progressive cell density: far-field (120-480 mm), intermediate domain ($\leqslant 60$ mm), near-body region ($\leqslant 30$ mm), and high-resolution zone ($\leqslant 15$ mm) surrounding the vehicle. Dedicated 6-layer boundary layer refinement with total thickness under 24 mm captures viscous phenomena. (b) Transverse section at $x = 3.12$ m demonstrates consistent refinement strategy with graduated cell density approaching vehicle surfaces, enabling accurate wake structure resolution while maintaining computational efficiency.

3.2 Mesh Generation

Our automated mesh generation workflow consists of two sequential stages: surface wrapping and volume mesh generation.

Surface Wrapping Morphed geometries frequently exhibit topological defects, including mesh intersections and open edges, requiring systematic resolution. We employed STAR-CCM+®'s surface wrapping functionality on individual components—vehicle body, drivetrain, engine compartment, wheels, and coolers—to ensure simulation-ready geometry. Critical regions with fine features, particularly drivetrain and grille openings, received 10% relative size refinement and specialized contact prevention parameters to maintain geometric fidelity while eliminating surface intersections. Each component underwent independent wrapping before integration into the computational domain. Complete technical specifications are detailed in Section C.2.

Volume Mesh Generation Our volume mesh (Figure 4) employs refinement strategies aligned with validated practices (Heft et al., 2012; Zhang et al., 2019) using STAR-CCM+®'s production-grade algorithms. Each simulation domain comprises approximately 12 million hexahedral-dominant cells with strategic density distribution targeting aerodynamically significant features. The meshing protocol incorporates high-resolution prismatic boundary layers on all vehicle surfaces—both external and internal—ensuring proper resolution of boundary phenomena including separation, reattachment, and near-wall flow structures. To maintain dataset consistency, we automated the entire meshing sequence through Java macros with identical parameters across all 12,000 simulations. Additional details are provided in Section C.3.

3.3 Industrial-grade Simulation

Computational Domain and Boundary Conditions Our framework implements automotive industry-standard simulation protocols using a domain extending 15 vehicle lengths streamwise, 10 widths laterally, and 12 heights vertically. The inlet boundary, positioned three vehicle lengths upstream, imposes $40\,\mathrm{m/s}$ ($144\,\mathrm{km/h}$) freestream velocity with 1% turbulence intensity generated through spectral synthesizer algorithms. The downstream boundary enforces zero-gradient pressure outlet conditions. Vehicle-ground interaction employs sliding wall boundaries with rotating reference frames, calculating wheel angular velocity ($\omega = u_\infty/r$) based on instantaneous tire geometry. The engine compartment thermal management system incorporates experimentally validated porous media models with 0.6 porosity. All simulations utilize T/CSAE112-2019 standard atmospheric conditions: air density $\rho = 1.225\,\mathrm{kg/m^3}$ and dynamic viscosity $\mu = 1.855\,08 \times 10^{-5}\,\mathrm{Pa \cdot s}$.

Flow Physics Modeling Simulations solve 3D steady-state Reynolds-Averaged Navier–Stokes (RANS) equations (Reynolds, 1895) for incompressible flow with comprehensive wall distance modeling. We employed Shear-Stress Transport (SST) (Menter, 1994) k-ω turbulence formulation, selected for demonstrated accuracy in predicting flow separation and reattachment phenomena critical to automotive aerodynamics. Our hybrid all-y^+ wall treatment automatically transitions between direct viscous sublayer resolution and wall function approaches based on local mesh refinement, maintaining y^+ values below 200 while optimizing computational efficiency. Gradient reconstruction utilizes cell-based least squares minimization, ensuring numerical stability in regions with strong pressure gradients and separated flow. Complete governing equation formulations are provided in Section C.4.

Sovler Our solution strategy employs a pressure-based segregated solver with Semi-Implicit Method for Pressure-Linked Equations (SIMPLE) algorithm (Patankar and Spalding, 1983) for pressure-velocity coupling. Spatial discretization implements second-order schemes for pressure and momentum equations, with first-order upwind treatment for turbulence quantities, enhancing stability. Linear equation systems are resolved using Algebraic Multigrid (AMG) methods (Xu and Zikatanov, 2017) with V-cycle iterations (1 pre/post-sweep), achieving convergence to residuals below 10^{-5} within 30 iterations per time step. Carefully calibrated under-relaxation factors (0.7 for velocity, 0.8 for turbulence quantities) balance convergence rate with solution stability. Gauss-Seidel relaxation enhances iterative efficiency, particularly in high-gradient regions such as wheel wells and underbody flow channels.

3.4 Experimental Validation

Wind Tunnel Validation We validated our simulation methodology against high-fidelity measurements from Loughborough University Large Wind Tunnel facility (Johl et al., 2004), focusing on drag coefficient (C_D)—the critical automotive aerodynamics performance metric. Our 25%-scale simulations precisely matched physical models provided by FKFS Stuttgart, ensuring geometric consistency between computational and experimental configurations. As shown in Table 2, simulations demonstrate exceptional agreement with experimental measurements across all three rear body configurations (Fastback, Notchback, Estateback), achieving 1.04% average relative deviation with maximum discrepancy below 1.8%. This correlation substantiates our simulation methodology's predictive accuracy for aerodynamic performance assessment. Detailed convergence analysis and mesh independence studies are presented in Section C.7.

Table 2: **Data scaling effects on drag coefficient prediction accuracy.** Transolver model performance analysis with increasing training sample size. Left and center: Scatter plots of predicted versus ground truth C_D values for models trained on 400 and 1200 samples, respectively, with diagonal green line representing perfect prediction ($y = x$) and red regression line showing actual prediction trends with correlation coefficients. Right: Violin plots comparing prediction error distributions, demonstrating improved performance with increased data volume (mean absolute error decreasing from 2.99% to 2.78%). Results confirm `DrivAerStar`'s effective learning scaling properties and potential for further accuracy improvements with additional training data. Comprehensive scaling results across all configurations are detailed in Section D.2.

Rear Configuration	**Wind Tunnel** C_D	`DrivAerStar` C_D	**Deviation (%)**
FastBack	0.278	0.2749	1.12%
NotchBack	0.279	0.2767	0.82%
Estateback	0.299	0.2955	1.17%

PIV Validation Flow structure prediction was further validated through Particle Image Velocimetry (PIV) measurements in aerodynamically critical regions—front stagnation zones, A-pillar vortices, and rear wake structures. Surface pressure distributions were compared using data from 60 strategically positioned pressure taps, emphasizing the interchangeable rear configurations. As visualized in Figure 5, these comparisons demonstrate excellent agreement in both magnitude and spatial distribution of pressure coefficients and velocity fields. The observed congruence confirms that our dataset accurately captures complex aerodynamic phenomena governing vehicle performance, including internal engine bay flows typically omitted in simplified models. Quantitative simulation-experiment difference analysis is provided in Section C.8.

 https://doi.org/10.52202/085713-3293

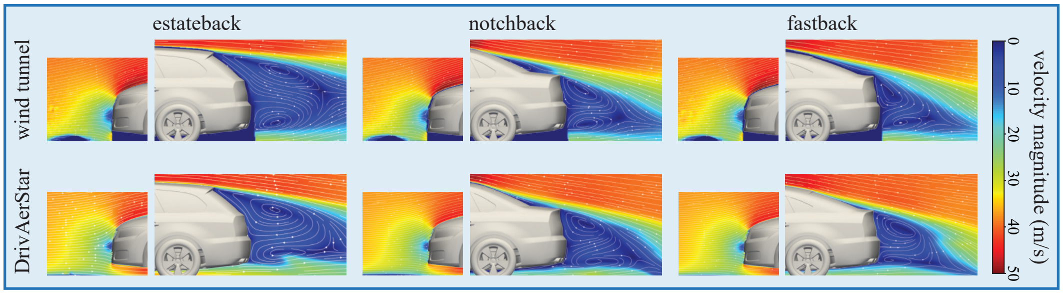

(a) wake and stagnation regime by PIV images

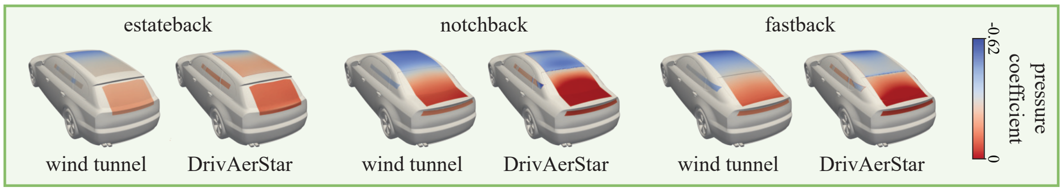

(b) time-averaged C_P

Figure 5: **Validation of flow physics predictions against wind tunnel measurements.** (a) Velocity magnitude distributions compare wind tunnel PIV measurements (top row) with `DrivAerStar` predictions (bottom row) in wake regions and stagnation zones, demonstrating excellent flow structure agreement. (b) Surface pressure coefficient (C_P) distributions across vehicle body surfaces show consistent prediction accuracy between experimental and computational results for all three vehicle configurations, confirming accurate capture of complex aerodynamic phenomena.

4 Benchmarks on `DrivAerStar`

4.1 Experimental Setup

Benchmark Objectives We establish comprehensive machine learning benchmarks on the `DrivAerStar` dataset to evaluate its industrial relevance and predictive capability. These benchmarks assess state-of-the-art deep learning architectures on aerodynamic prediction tasks using high-fidelity CFD data representative of real automotive development. The primary task involves predicting surface pressure ($\tilde{p}$) and wall shear stress ($\tilde{\tau}_w$) distributions from vehicle geometry, as well as the derived drag coefficients (C_D). This setup aligns with recent advances in automotive aerodynamics machine learning research (Hao et al., 2023; Wu et al., 2024; Nabian et al., 2024; Choy et al., 2025; Liu et al., 2025; Bleeker et al., 2025) while providing realistic validation through our industry-standard dataset.

Dataset Configurations We systematically evaluated dataset scale and diversity effects. Initial benchmarks used restricted training sets (400-1200 samples) from single vehicle configurations (Estateback), while advanced experiments incorporated multi-configuration datasets spanning all three rear body types (Fastback, Estateback, Notchback). All experiments maintained consistent validation and test splits with 150 cases per configuration type. Additional experimental details are provided in Section F.

Evaluation Protocol Model performance evaluation ensures accurate local flow physics representation and reliable global performance prediction—essential requirements for industrial applications. For spatial distribution accuracy of surface fields, we employ the relative L_2 error. Each flow field variable ϕ (*e.g.*, velocity, pressure) is standardized via mean (μ_ϕ) and standard deviation (σ_ϕ) computed from dataset samples (*i.e.*, $\hat{\phi} = \frac{\phi-\mu_\phi}{\sigma_\phi}$): $\epsilon = \frac{||\hat{\phi}_{\text{pred}}-\hat{\phi}_{\text{true}}||_2}{||\hat{\phi}_{\text{true}}||_2}$, eliminating scale discrepancies among variables, where $\hat{\phi}_{\text{pred}}$ and $\hat{\phi}_{\text{true}}$ denote standardized predicted and ground-truth flow field variables, respectively. For integrated quantities (*e.g.*, drag coefficient C_D), we assess absolute and percentage errors to ensure correct global performance prediction. Complete metric definitions and standardization procedures are provided in Section D.1.

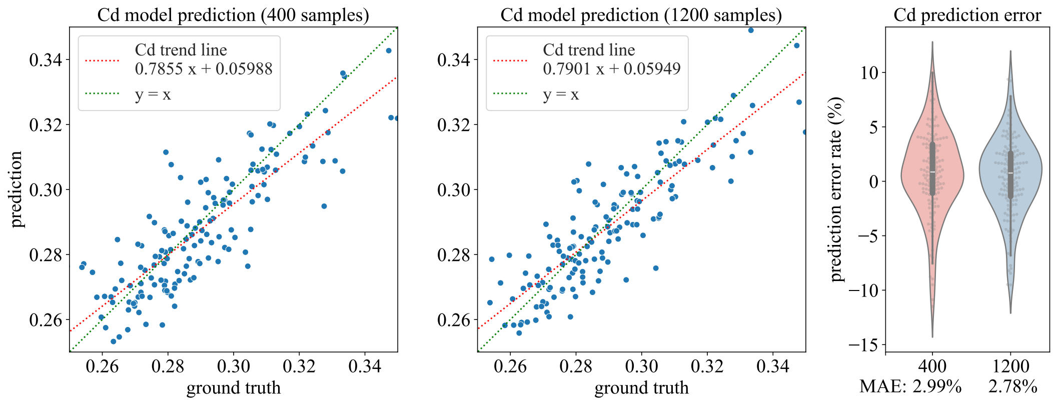

Figure 6: **Data scaling effects on drag coefficient prediction accuracy.** Analysis of Transolver model performance with increasing training sample size. Left and center: Scatter plots of predicted versus ground truth C_D values for models trained on 400 and 1200 samples, respectively. The diagonal green line represents perfect prediction ($y = x$), while the red regression line shows the actual prediction trend with correlation coefficients. Right: Violin plots comparing prediction error distributions, showing improved performance with increased data volume (mean absolute error decreasing from 2.99% to 2.78%). This demonstrates the dataset's effective learning scaling properties and potential for further accuracy improvements with additional samples. Comprehensive scaling results across all configurations are provided in Section D.2.

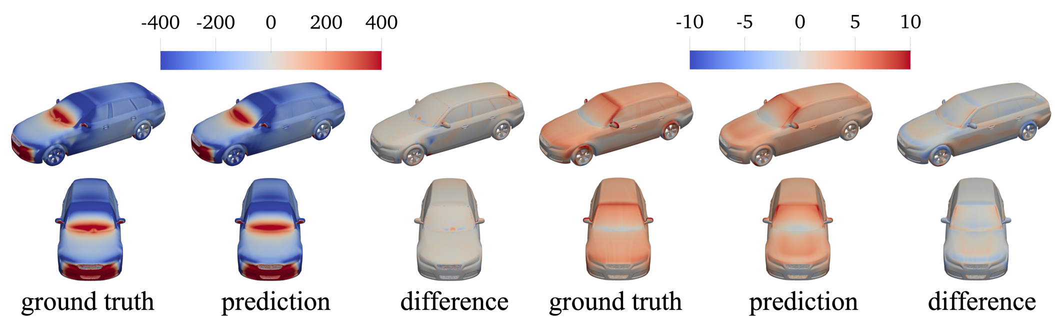

(a) surface pressure (Pa) (b) wall shear stress (x) (Pa)

Figure 7: **Surface field prediction accuracy across critical aerodynamic regions.** (a) Surface pressure distributions (Pa) comparing ground truth CFD simulation (left), neural network prediction (middle), and point-wise difference (right). (b) Wall shear stress τ_x (Pa) in streamwise direction with ground truth (left), model prediction (middle), and prediction error (right). The model accurately captures high-gradient regions around A-pillars and wheel wells while maintaining precision in uniform flow areas, demonstrating robust performance across diverse aerodynamic phenomena.

4.2 Results

Surface Field Prediction We evaluated three state-of-the-art deep learning architectures on `DrivAerStar` for predicting surface pressure and wall shear stress fields, as well as the derived drag coefficients. The performance metrics on the test set are summarized in Table A2.

Each model was trained on both specialized single-configuration subsets (Estateback only) and the complete multi-configuration dataset (Fastback, Notchback, and Estateback). Results consistently showed higher prediction errors on the complete dataset, confirming that morphological diversity significantly increases prediction complexity. This performance differential quantifies the fundamental trade-off between prediction accuracy and geometric variability in aerodynamic machine learning tasks. Representative prediction visualizations are presented in Figure 7.

Data Scaling Analysis To investigate model generalization capabilities and data efficiency, we conducted systematic scaling experiments following `DrivAer` protocols. Both single-configuration subsets and complete datasets were divided into training (80%) and test (20%) partitions, with progressive increases in training samples while maintaining consistent test evaluation. The resulting learning curves (Figure 6) reveal characteristic scaling behaviors for each architecture and quantify data requirements for achieving specific prediction accuracy thresholds.

https://doi.org/10.52202/085713-3293

Table 3: **Drag coefficient prediction scaling analysis in multi-vehicle configurations.** Transolver model performance across varying training dataset sizes (400–12,000 samples) evaluated on a consistent validation set of 150 samples per vehicle configuration. Learning curves demonstrate systematic improvement in C_D prediction accuracy with increased training data, confirming the dataset's scalability and the model's ability to leverage additional samples for enhanced aerodynamic performance prediction across diverse vehicle geometries.

Metrics	**400**	**800**	**1,200**	**12,000**
C_D validation loss	0.0375	0.0335	0.0286	0.0266
Improvement	-	10.67%	23.73%	29.07%

We further assessed training size effects on Transolver's predictive performance for drag coefficient (C_D)—a key CFD metric for vehicle aerodynamic optimization—in multi-vehicle settings. Results including C_D validation loss and relative improvement values are summarized in Table 3. Raw scaling experiment data (loss curves, test sample distributions) are provided in Section D.3.

5 Conclusion

We present `DrivAerStar`, a comprehensive automotive aerodynamics dataset comprising 12,000 high-fidelity CFD simulations that bridges the gap between academic research and industrial applications. Generated using industry-standard STAR-CCM+® software across three rear body configurations with 20 systematically varied CAD parameters, `DrivAerStar` represents the most comprehensive and validated automotive aerodynamics dataset to date.

Our key contributions establish new standards for CFD datasets in automotive engineering. We provide the highest-fidelity geometric representations available, incorporating complete engine compartments, cooling systems, and drivetrain components typically omitted in simplified academic models. The systematic parametric morphing using FFD techniques creates geometric diversity while maintaining industrial relevance. Our rigorous experimental validation against wind tunnel measurements achieves exceptional accuracy with 1.04% mean relative error for drag coefficients and excellent agreement in PIV flow field comparisons, establishing confidence in the dataset's predictive capability for real-world applications.

The industrial-grade simulation methodology employs production-level meshing protocols with 12 million hexahedral-dominant cells per case, capturing boundary layer phenomena and separation dynamics critical to automotive aerodynamics. Our comprehensive data formats provide complete access to flow physics information. The resulting 20TB dataset includes pressure coefficients, wall shear stress, velocity fields, streamlines, and iso-surfaces, enabling diverse research applications from fundamental flow physics to applied design optimization.

Our extensive machine learning benchmarks demonstrate that models trained on `DrivAerStar` achieve industrial-grade prediction accuracy while reducing computational costs by orders of magnitude compared to traditional CFD approaches. The systematic evaluation reveals fundamental trade-offs between geometric variability and prediction accuracy, providing crucial insights for developing robust aerodynamic prediction models and guiding future dataset development efforts.

`DrivAerStar`'s impact extends beyond immediate research applications to enable transformative changes in automotive development processes. By providing validated, high-fidelity training data, we enable the development of fast, accurate surrogate models that can replace computationally expensive CFD simulations in design optimization loops. This supports rapid design exploration, real-time performance assessment, and integration of aerodynamic considerations throughout the vehicle development cycle.

The open availability of `DrivAerStar` under permissive licensing, combined with comprehensive documentation and reproducible workflows, establishes a foundation for collaborative research in automotive aerodynamics. Future extensions will address current limitations, including multidisciplinary coupling with thermal management and structural dynamics, detailed in Section G.

By democratizing access to industrial-quality aerodynamic data, `DrivAerStar` empowers researchers worldwide to develop next-generation computational methods that accelerate the transition to more efficient, sustainable automotive designs. This work represents a critical step toward data-driven automotive engineering, where machine learning and high-fidelity simulation combine to revolutionize vehicle development practices.

Acknowledgments and Disclosure of Funding

Deep learning experiments were conducted using the PaddlePaddle framework. We gratefully acknowledge Siemens Digital Industries Software for granting an educational-discount license of STAR-CCM+® to Peking University, enabling part of the CFD simulations presented in this study. Y. Xu, L. Cui, and Y. Zhu were supported by the National Natural Science Foundation of China (62376009), the PKU-BingJi Joint Laboratory for Artificial Intelligence, and the National Comprehensive Experimental Base for Governance of Intelligent Society, Wuhan East Lake High-Tech Development Zone.

References

Abinesh, J. and Arunkumar, J. (2014). Cfd analysis of aerodynamic drag reduction and improve fuel economy. *International Journal of Mechanical Engineering and Robotics Research*, 3(4):430. 1

Ashton, N., Angel, J., Ghate, A., Kenway, G., Wong, M. L., Kiris, C., Walle, A., Maddix, D., and Page, G. (2024a). Windsorml: High-fidelity computational fluid dynamics dataset for automotive aerodynamics. In *Proceedings of Advances in Neural Information Processing Systems (NeurIPS)*. 3

Ashton, N., Maddix, D. C., Gundry, S., and Shabestari, P. M. (2024b). Ahmedml: High-fidelity computational fluid dynamics dataset for incompressible, low-speed bluff body aerodynamics. 4

Ashton, N., Mockett, C., Fuchs, M., Fliessbach, L., Hetmann, H., Knacke, T., Schonwald, N., Skaperdas, V., Fotiadis, G., Walle, A., et al. (2024c). Drivaerml: High-fidelity computational fluid dynamics dataset for road-car external aerodynamics. 2, 3, A12

Bibra, E. M., Connelly, E., Dhir, S., Drtil, M., Henriot, P., Hwang, I., Le Marois, J.-B., McBain, S., Paoli, L., and Teter, J. (2022). Global ev outlook 2022: Securing supplies for an electric future. Technical report, IEA. 1

Bjerkan, K. Y., Nørbech, T. E., and Nordtømme, M. E. (2016). Incentives for promoting battery electric vehicle (bev) adoption in norway. *Transportation Research Part D: Transport and Environment*, 43:169–180. 2

Bleeker, M., Dorfer, M., Kronlachner, T., Sonnleitner, R., Alkin, B., and Brandstetter, J. (2025). Neuralcfd: Deep learning on high-fidelity automotive aerodynamics simulations. 8

Bonnet, F., Mazari, J., Cinnella, P., and Gallinari, P. (2022). Airfrans: High fidelity computational fluid dynamics dataset for approximating reynolds-averaged navier–stokes solutions. In *Proceedings of Advances in Neural Information Processing Systems (NeurIPS)*. 3

Brandt, A., Jacobson, B., and Sebben, S. (2022). High speed driving stability of road vehicles under crosswinds: an aerodynamic and vehicle dynamic parametric sensitivity analysis. *Vehicle System Dynamics*, 60(7):2334–2357. 1

Choy, C., Kamenev, A., Kossaifi, J., Rietmann, M., Kautz, J., and Azizzadenesheli, K. (2025). Factorized implicit global convolution for automotive computational fluid dynamics prediction. 8

Chung, W. T., Akoush, B., Sharma, P., Tamkin, A., Jung, K. S., Chen, J., Guo, J., Brouzet, D., Talei, M., Savard, B., et al. (2023). Turbulence in focus: Benchmarking scaling behavior of 3d volumetric super-resolution with blastnet 2.0 data. In *Proceedings of Advances in Neural Information Processing Systems (NeurIPS)*. 3

Chung, W. T., Jung, K. S., Chen, J. H., and Ihme, M. (2022). Blastnet: A call for community-involved big data in combustion machine learning. *Applications in Energy and Combustion Science*, 12:100087. 3

Cobb, A., Roy, A., Elenius, D., Heim, F., Swenson, B., Whittington, S., Walker, J., Bapty, T., Hite, J., Ramani, K., et al. (2023). Aircraftverse: a large-scale multimodal dataset of aerial vehicle designs. In *Proceedings of Advances in Neural Information Processing Systems (NeurIPS)*. 3

 https://doi.org/10.52202/085713-3293

Elrefaie, M., Dai, A., and Ahmed, F. (2025). Drivaernet: A parametric car dataset for data-driven aerodynamic design and prediction. *Journal of Mechanical Design*, 147(4). 4

Elrefaie, M., Morar, F., Dai, A., and Ahmed, F. (2024). Drivaernet++: A large-scale multimodal car dataset with computational fluid dynamics simulations and deep learning benchmarks. In *Proceedings of Advances in Neural Information Processing Systems (NeurIPS)*. 2, 3, 4, A12

Gao, Q., Pan, S., Wang, H., Wei, R., and Wang, J. (2021). Particle reconstruction of volumetric particle image velocimetry with the strategy of machine learning. *Advances in Aerodynamics*, 3(1):28. 3

Hannan, M. A., Azidin, F., and Mohamed, A. (2014). Hybrid electric vehicles and their challenges: A review. *Renewable and Sustainable Energy Reviews*, 29:135–150. 2

Hao, Z., Wang, Z., Su, H., Ying, C., Dong, Y., Liu, S., Cheng, Z., Song, J., and Zhu, J. (2023). Gnot: A general neural operator transformer for operator learning. In *Proceedings of International Conference on Machine Learning (ICML)*. 2, 8, A13

Hassan, S. M. S., Feeney, A., Dhruv, A., Kim, J., Suh, Y., Ryu, J., Won, Y., and Chandramowlishwaran, A. (2023). Bubbleml: A multiphase multiphysics dataset and benchmarks for machine learning. In *Proceedings of Advances in Neural Information Processing Systems (NeurIPS)*. 3

Heft, A. I., Indinger, T., and Adams, N. A. (2012). Experimental and numerical investigation of the drivaer model. In *Fluids Engineering Division Summer Meeting*. 5, 6

Huluka, A. and Kim, C. (2019). Numerical study on aerodynamic drag reduction and energy harvest for electric vehicle: a concept to extend driving range. In *IOP Conference Series: Materials Science and Engineering*. 1

Johl, G., Passmore, M., and Render, P. (2004). Design methodology and performance of an indraft wind tunnel. *The Aeronautical Journal*, 108(1087):465–473. 7

Kochkov, D., Smith, J. A., Alieva, A., Wang, Q., Brenner, M. P., and Hoyer, S. (2021). Machine learning–accelerated computational fluid dynamics. *Proceedings of the National Academy of Sciences (PNAS)*, 118(21):e2101784118. 3

Li, Z., Kovachki, N. B., Choy, C., Li, B., Kossaifi, J., Otta, S. P., Nabian, M. A., Stadler, M., Hundt, C., Azizzadenesheli, K., and Anandkumar, A. (2023). Geometry-informed neural operator for large-scale 3d pdes. In *Proceedings of Advances in Neural Information Processing Systems (NeurIPS)*. 4

Liu, P., Wang, P., Ren, X., Yuan, H., Hao, Z., Xu, C., Cai, S., and Ni, D. (2025). Aerogto: An efficient graph-transformer operator for learning large-scale aerodynamics of 3d vehicle geometries. In *Proceedings of AAAI Conference on Artificial Intelligence (AAAI)*. 8

Lu, L., Jin, P., Pang, G., Zhang, Z., and Karniadakis, G. E. (2021). Learning nonlinear operators via deeponet based on the universal approximation theorem of operators. *Nature machine intelligence*, 3(3):218–229. 3

Menter, F. R. (1994). Two-equation eddy-viscosity turbulence models for engineering applications. *AIAA Journal*, 32(8):1598–1605. 6, A7

Nabian, M. A., Liu, C., Ranade, R., and Choudhry, S. (2024). X-meshgraphnet: Scalable multi-scale graph neural networks for physics simulation. 8

Patankar, S. V. and Spalding, D. B. (1983). A calculation procedure for heat, mass and momentum transfer in three-dimensional parabolic flows. In *Numerical prediction of flow, heat transfer, turbulence and combustion*, pages 54–73. Elsevier. 7

Payri, F., Luján, J. M., Guardiola, C., and Pla, B. (2015). A challenging future for the ic engine: new technologies and the control role. *Oil & Gas Science and Technology–Revue d'IFP Energies nouvelles*, 70(1):15–30. 2

Qi, C. R., Su, H., Mo, K., and Guibas, L. J. (2017). Pointnet: Deep learning on point sets for 3d classification and segmentation. In *Proceedings of Conference on Computer Vision and Pattern Recognition (CVPR)*. 2, A12

Raissi, M., Perdikaris, P., and Karniadakis, G. E. (2019). Physics-informed neural networks: A deep learning framework for solving forward and inverse problems involving nonlinear partial differential equations. *Journal of Computational physics*, 378:686–707. 3

Reynolds, O. (1895). On the dynamical theory of incompressible viscous fluids and the determination of the criterion. *Philosophical Transactions of the Royal Society of London (A)*, 186:123–164. 6

Schlichting, H. and Kestin, J. (1961). *Boundary layer theory*, volume 121. Springer. 2

Song, B., Yuan, C., Permenter, F., Arechiga, N., and Ahmed, F. (2023). Surrogate modeling of car drag coefficient with depth and normal renderings. In *International Design Engineering Technical Conferences and Computers and Information in Engineering Conference*. 3

Spalart, P. R. and Rumsey, C. L. (2007). Effective inflow conditions for turbulence models in aerodynamic calculations. *AIAA journal*, 45(10):2544–2553. A7

Strangfeld, C., Wieser, D., Schmidt, H.-J., Woszidlo, R., Nayeri, C., and Paschereit, C. (2013). Experimental study of baseline flow characteristics for the realistic car model drivaer. Technical report, SAE Technical Paper. 5

Stüben, K. (2001). A review of algebraic multigrid. *Numerical Analysis: Historical Developments in the 20th Century*, pages 331–359. A8

Takamoto, M., Praditia, T., Leiteritz, R., MacKinlay, D., Alesiani, F., Pflüger, D., and Niepert, M. (2022). Pdebench: An extensive benchmark for scientific machine learning. In *Proceedings of Advances in Neural Information Processing Systems (NeurIPS)*. 3

Tang, H., Wang, Y., Wang, T., and Tian, L. (2023). Discovering explicit reynolds-averaged turbulence closures for turbulent separated flows through deep learning-based symbolic regression with non-linear corrections. *Physics of Fluids*, 35(2). 3

Toshev, A., Galletti, G., Fritz, F., Adami, S., and Adams, N. (2023). Lagrangebench: A lagrangian fluid mechanics benchmarking suite. In *Proceedings of Advances in Neural Information Processing Systems (NeurIPS)*. 3

Umetani, N. and Bickel, B. (2018). Learning three-dimensional flow for interactive aerodynamic design. *ACM Transactions on Graphics (TOG)*, 37(4):1–10. 3

Upadhyaya, A. and Mahanta, C. (2023). An overview of battery based electric vehicle technologies with emphasis on energy sources, their configuration topologies and management strategies. *IEEE Transactions on Intelligent Transportation Systems*, 25(2):1087–1111. 2

Varney, M., Passmore, M., Wittmeier, F., and Kuthada, T. (2020). Experimental data for the validation of numerical methods: Drivaer model. *Fluids*, 5(4):236. 2

Wang, Y., Zhen, X., Wu, J., Gu, Z., Xiao, Z., and Yang, X. (2013). Hybrid cfd/fem-bem simulation of cabin aerodynamic noise for vehicles traveling at high speed. *Science China Technological Sciences*, 56:1697–1708. 1

Warner, J. and Emory, M. (2025). Introducing luminary shift models: A suite of physics ai foundation models to transform engineering design. Technical report, Luminary Cloud. 4

Wu, H., Luo, H., Wang, H., Wang, J., and Long, M. (2024). Transolver: A fast transformer solver for pdes on general geometries. In *Proceedings of International Conference on Machine Learning (ICML)*. 2, 8, A12

Xu, J. and Zikatanov, L. (2017). Algebraic multigrid methods. *Acta Numerica*, 26:591–721. 7

Zhang, C., Bounds, C. P., Foster, L., and Uddin, M. (2019). Turbulence modeling effects on the cfd predictions of flow over a detailed full-scale sedan vehicle. *Fluids*, 4(3):148. 6

 https://doi.org/10.52202/085713-3293

NeurIPS Paper Checklist

1. **Claims**

   Question: Do the main claims made in the abstract and introduction accurately reflect the paper's contributions and scope?

   Answer: [Yes]

   Justification: Yes, the main claims made in the abstract and introduction accurately reflect our contribution and scope, which is the comprehensive, reproducible, and industrial-grade dataset `DrivAerStar`.

   Guidelines:

   - The answer NA means that the abstract and introduction do not include the claims made in the paper.
   - The abstract and/or introduction should clearly state the claims made, including the contributions made in the paper and important assumptions and limitations. A No or NA answer to this question will not be perceived well by the reviewers.
   - The claims made should match theoretical and experimental results, and reflect how much the results can be expected to generalize to other settings.
   - It is fine to include aspirational goals as motivation as long as it is clear that these goals are not attained by the paper.

2. **Limitations**

   Question: Does the paper discuss the limitations of the work performed by the authors?

   Answer: [Yes]

   Justification: We have discussed the limitations in Section G, including insufficient geometric deformation to cover all designs in actual industrial development, and the CFD solver may still deviate from the real-industry conditions.

   Guidelines:

   - The answer NA means that the paper has no limitation while the answer No means that the paper has limitations, but those are not discussed in the paper.
   - The authors are encouraged to create a separate "Limitations" section in their paper.
   - The paper should point out any strong assumptions and how robust the results are to violations of these assumptions (*e.g.*, independence assumptions, noiseless settings, model well-specification, asymptotic approximations only holding locally). The authors should reflect on how these assumptions might be violated in practice and what the implications would be.
   - The authors should reflect on the scope of the claims made, *e.g.*, if the approach was only tested on a few datasets or with a few runs. In general, empirical results often depend on implicit assumptions, which should be articulated.
   - The authors should reflect on the factors that influence the performance of the approach. For example, a facial recognition algorithm may perform poorly when image resolution is low or images are taken in low lighting. Or a speech-to-text system might not be used reliably to provide closed captions for online lectures because it fails to handle technical jargon.
   - The authors should discuss the computational efficiency of the proposed algorithms and how they scale with dataset size.
   - If applicable, the authors should discuss possible limitations of their approach to address problems of privacy and fairness.
   - While the authors might fear that complete honesty about limitations might be used by reviewers as grounds for rejection, a worse outcome might be that reviewers discover limitations that aren't acknowledged in the paper. The authors should use their best judgment and recognize that individual actions in favor of transparency play an important role in developing norms that preserve the integrity of the community. Reviewers will be specifically instructed to not penalize honesty concerning limitations.

3. **Theory assumptions and proofs**

Question: For each theoretical result, does the paper provide the full set of assumptions and a complete (and correct) proof?

Answer: [Yes]

Justification: We have provided a detailed explanation of the foundational theories of fluid dynamics and a thorough simulation setup clarification according to the theories, which can be found at Section C.4.

Guidelines:

- The answer NA means that the paper does not include theoretical results.
- All the theorems, formulas, and proofs in the paper should be numbered and cross-referenced.
- All assumptions should be clearly stated or referenced in the statement of any theorems.
- The proofs can either appear in the main paper or the supplemental material, but if they appear in the supplemental material, the authors are encouraged to provide a short proof sketch to provide intuition.
- Inversely, any informal proof provided in the core of the paper should be complemented by formal proofs provided in appendix or supplemental material.
- Theorems and Lemmas that the proof relies upon should be properly referenced.

4. **Experimental result reproducibility**

   Question: Does the paper fully disclose all the information needed to reproduce the main experimental results of the paper to the extent that it affects the main claims and/or conclusions of the paper (regardless of whether the code and data are provided or not)?

   Answer: [Yes]

   Justification: We provide the implementation details of the data generation pipeline at Sections 3 and C.

   Guidelines:

   - The answer NA means that the paper does not include experiments.
   - If the paper includes experiments, a No answer to this question will not be perceived well by the reviewers: Making the paper reproducible is important, regardless of whether the code and data are provided or not.
   - If the contribution is a dataset and/or model, the authors should describe the steps taken to make their results reproducible or verifiable.
   - Depending on the contribution, reproducibility can be accomplished in various ways. For example, if the contribution is a novel architecture, describing the architecture fully might suffice, or if the contribution is a specific model and empirical evaluation, it may be necessary to either make it possible for others to replicate the model with the same dataset, or provide access to the model. In general. releasing code and data is often one good way to accomplish this, but reproducibility can also be provided via detailed instructions for how to replicate the results, access to a hosted model (*e.g.*, in the case of a large language model), releasing of a model checkpoint, or other means that are appropriate to the research performed.
   - While NeurIPS does not require releasing code, the conference does require all submissions to provide some reasonable avenue for reproducibility, which may depend on the nature of the contribution. For example
     (a) If the contribution is primarily a new algorithm, the paper should make it clear how to reproduce that algorithm.
     (b) If the contribution is primarily a new model architecture, the paper should describe the architecture clearly and fully.
     (c) If the contribution is a new model (*e.g.*, a large language model), then there should either be a way to access this model for reproducing the results or a way to reproduce the model (*e.g.*, with an open-source dataset or instructions for how to construct the dataset).

https://doi.org/10.52202/085713-3293

(d) We recognize that reproducibility may be tricky in some cases, in which case authors are welcome to describe the particular way they provide for reproducibility. In the case of closed-source models, it may be that access to the model is limited in some way (*e.g.*, to registered users), but it should be possible for other researchers to have some path to reproducing or verifying the results.

5. **Open access to data and code**

   Question: Does the paper provide open access to the data and code, with sufficient instructions to faithfully reproduce the main experimental results, as described in supplemental material?

   Answer: [Yes]

   Justification: Both `DrivAerStar` and code for data processing and benchmarking are accessible via our project homepage. We provide the detailed instructions for our dataset and code on the related websites.

   Guidelines:

   - The answer NA means that paper does not include experiments requiring code.
   - Please see the NeurIPS code and data submission guidelines (`https://nips.cc/public/guides/CodeSubmissionPolicy`) for more details.
   - While we encourage the release of code and data, we understand that this might not be possible, so "No" is an acceptable answer. Papers cannot be rejected simply for not including code, unless this is central to the contribution (*e.g.*, for a new open-source benchmark).
   - The instructions should contain the exact command and environment needed to run to reproduce the results. See the NeurIPS code and data submission guidelines (`https://nips.cc/public/guides/CodeSubmissionPolicy`) for more details.
   - The authors should provide instructions on data access and preparation, including how to access the raw data, preprocessed data, intermediate data, and generated data, etc.
   - The authors should provide scripts to reproduce all experimental results for the new proposed method and baselines. If only a subset of experiments are reproducible, they should state which ones are omitted from the script and why.
   - At submission time, to preserve anonymity, the authors should release anonymized versions (if applicable).
   - Providing as much information as possible in supplemental material (appended to the paper) is recommended, but including URLs to data and code is permitted.

6. **Experimental setting/details**

   Question: Does the paper specify all the training and test details (*e.g.*, data splits, hyperparameters, how they were chosen, type of optimizer, etc.) necessary to understand the results?

   Answer: [Yes]

   Justification: We have made clear the dataset generation settings, reported how we validate and benchmark the SOTA models. More details can be found in the Sections D.2 and F.

   Guidelines:

   - The answer NA means that the paper does not include experiments.
   - The experimental setting should be presented in the core of the paper to a level of detail that is necessary to appreciate the results and make sense of them.
   - The full details can be provided either with the code, in appendix, or as supplemental material.

7. **Experiment statistical significance**

   Question: Does the paper report error bars suitably and correctly defined or other appropriate information about the statistical significance of the experiments?

   Answer: [No]

   Justification: Due to computational resource constraints, we were unable to establish the statistical significance of our experimental results.

Guidelines:

- The answer NA means that the paper does not include experiments.
- The authors should answer "Yes" if the results are accompanied by error bars, confidence intervals, or statistical significance tests, at least for the experiments that support the main claims of the paper.
- The factors of variability that the error bars are capturing should be clearly stated (for example, train/test split, initialization, random drawing of some parameter, or overall run with given experimental conditions).
- The method for calculating the error bars should be explained (closed form formula, call to a library function, bootstrap, etc.)
- The assumptions made should be given (*e.g.*, Normally distributed errors).
- It should be clear whether the error bar is the standard deviation or the standard error of the mean.
- It is OK to report 1-sigma error bars, but one should state it. The authors should preferably report a 2-sigma error bar than state that they have a 96% CI, if the hypothesis of Normality of errors is not verified.
- For asymmetric distributions, the authors should be careful not to show in tables or figures symmetric error bars that would yield results that are out of range (*e.g.* negative error rates).
- If error bars are reported in tables or plots, The authors should explain in the text how they were calculated and reference the corresponding figures or tables in the text.

8. **Experiments compute resources**

   Question: For each experiment, does the paper provide sufficient information on the computer resources (type of compute workers, memory, time of execution) needed to reproduce the experiments?

   Answer: [Yes]

   Justification: We have stated the high-performance computation cluster configuration and CPU core-hours needed in this paper to produce `DrivAerStar` in Section C.5.

   Guidelines:

   - The answer NA means that the paper does not include experiments.
   - The paper should indicate the type of compute workers CPU or GPU, internal cluster, or cloud provider, including relevant memory and storage.
   - The paper should provide the amount of compute required for each of the individual experimental runs as well as estimate the total compute.
   - The paper should disclose whether the full research project required more compute than the experiments reported in the paper (*e.g.*, preliminary or failed experiments that didn't make it into the paper).

9. **Code of ethics**

   Question: Does the research conducted in the paper conform, in every respect, with the NeurIPS Code of Ethics https://neurips.cc/public/EthicsGuidelines?

   Answer: [Yes]

   Justification: We have adhered to the NeurIPS Code of Ethics throughout the entire process of our research.

   Guidelines:

   - The answer NA means that the authors have not reviewed the NeurIPS Code of Ethics.
   - If the authors answer No, they should explain the special circumstances that require a deviation from the Code of Ethics.
   - The authors should make sure to preserve anonymity (*e.g.*, if there is a special consideration due to laws or regulations in their jurisdiction).

10. **Broader impacts**

    Question: Does the paper discuss both potential positive societal impacts and negative societal impacts of the work performed?

https://doi.org/10.52202/085713-3293

Answer: [Yes]

Justification: We have stated that our work could bring positive societal impacts through boosting the automotive industry's development cycle and even extending beyond the field of automotive aerodynamics in Section B.

Guidelines:

- The answer NA means that there is no societal impact of the work performed.
- If the authors answer NA or No, they should explain why their work has no societal impact or why the paper does not address societal impact.
- Examples of negative societal impacts include potential malicious or unintended uses (*e.g.*, disinformation, generating fake profiles, surveillance), fairness considerations (*e.g.*, deployment of technologies that could make decisions that unfairly impact specific groups), privacy considerations, and security considerations.
- The conference expects that many papers will be foundational research and not tied to particular applications, let alone deployments. However, if there is a direct path to any negative applications, the authors should point it out. For example, it is legitimate to point out that an improvement in the quality of generative models could be used to generate deepfakes for disinformation. On the other hand, it is not needed to point out that a generic algorithm for optimizing neural networks could enable people to train models that generate Deepfakes faster.
- The authors should consider possible harms that could arise when the technology is being used as intended and functioning correctly, harms that could arise when the technology is being used as intended but gives incorrect results, and harms following from (intentional or unintentional) misuse of the technology.
- If there are negative societal impacts, the authors could also discuss possible mitigation strategies (*e.g.*, gated release of models, providing defenses in addition to attacks, mechanisms for monitoring misuse, mechanisms to monitor how a system learns from feedback over time, improving the efficiency and accessibility of ML).

11. **Safeguards**

Question: Does the paper describe safeguards that have been put in place for responsible release of data or models that have a high risk for misuse (*e.g.*, pretrained language models, image generators, or scraped datasets)?

Answer: [NA]

Justification: Our paper poses no risk since we have only collected data from credible sources.

Guidelines:

- The answer NA means that the paper poses no such risks.
- Released models that have a high risk for misuse or dual-use should be released with necessary safeguards to allow for controlled use of the model, for example by requiring that users adhere to usage guidelines or restrictions to access the model or implementing safety filters.
- Datasets that have been scraped from the Internet could pose safety risks. The authors should describe how they avoided releasing unsafe images.
- We recognize that providing effective safeguards is challenging, and many papers do not require this, but we encourage authors to take this into account and make a best faith effort.

12. **Licenses for existing assets**

Question: Are the creators or original owners of assets (*e.g.*, code, data, models), used in the paper, properly credited and are the license and terms of use explicitly mentioned and properly respected?

Answer: [Yes]

Justification: We've credited the owner of `DrivAer` assets and stated the licenses of software we used (STAR-CCM+® and Blender®) in the paper.

Guidelines:

- The answer NA means that the paper does not use existing assets.
- The authors should cite the original paper that produced the code package or dataset.
- The authors should state which version of the asset is used and, if possible, include a URL.
- The name of the license (*e.g.*, CC-BY 4.0) should be included for each asset.
- For scraped data from a particular source (*e.g.*, website), the copyright and terms of service of that source should be provided.
- If assets are released, the license, copyright information, and terms of use in the package should be provided. For popular datasets, `paperswithcode.com/datasets` has curated licenses for some datasets. Their licensing guide can help determine the license of a dataset.
- For existing datasets that are re-packaged, both the original license and the license of the derived asset (if it has changed) should be provided.
- If this information is not available online, the authors are encouraged to reach out to the asset's creators.

13. **New assets**

    Question: Are new assets introduced in the paper well documented and is the documentation provided alongside the assets?

    Answer: [Yes]

    Justification: Both `DrivAerStar` and code for data processing and benchmarking are well documented, and are accessible via our project homepage.

    Guidelines:

    - The answer NA means that the paper does not release new assets.
    - Researchers should communicate the details of the dataset/code/model as part of their submissions via structured templates. This includes details about training, license, limitations, etc.
    - The paper should discuss whether and how consent was obtained from people whose asset is used.
    - At submission time, remember to anonymize your assets (if applicable). You can either create an anonymized URL or include an anonymized zip file.

14. **Crowdsourcing and research with human subjects**

    Question: For crowdsourcing experiments and research with human subjects, does the paper include the full text of instructions given to participants and screenshots, if applicable, as well as details about compensation (if any)?

    Answer: [NA]

    Justification: This paper does not involve crowdsourcing nor research with human subjects.

    Guidelines:

    - The answer NA means that the paper does not involve crowdsourcing nor research with human subjects.
    - Including this information in the supplemental material is fine, but if the main contribution of the paper involves human subjects, then as much detail as possible should be included in the main paper.
    - According to the NeurIPS Code of Ethics, workers involved in data collection, curation, or other labor should be paid at least the minimum wage in the country of the data collector.

15. **Institutional review board (IRB) approvals or equivalent for research with human subjects**

    Question: Does the paper describe potential risks incurred by study participants, whether such risks were disclosed to the subjects, and whether Institutional Review Board (IRB) approvals (or an equivalent approval/review based on the requirements of your country or institution) were obtained?

    Answer: [NA]

https://doi.org/10.52202/085713-3293

Justification: This paper does not involve crowdsourcing nor research with human subjects.

Guidelines:

- The answer NA means that the paper does not involve crowdsourcing nor research with human subjects.
- Depending on the country in which research is conducted, IRB approval (or equivalent) may be required for any human subjects research. If you obtained IRB approval, you should clearly state this in the paper.
- We recognize that the procedures for this may vary significantly between institutions and locations, and we expect authors to adhere to the NeurIPS Code of Ethics and the guidelines for their institution.
- For initial submissions, do not include any information that would break anonymity (if applicable), such as the institution conducting the review.

16. **Declaration of LLM usage**

Question: Does the paper describe the usage of LLMs if it is an important, original, or non-standard component of the core methods in this research? Note that if the LLM is used only for writing, editing, or formatting purposes and does not impact the core methodology, scientific rigorousness, or originality of the research, declaration is not required.

Answer: [NA]

Justification: LLMs are not involved in our core method development in this research.

Guidelines:

- The answer NA means that the core method development in this research does not involve LLMs as any important, original, or non-standard components.
- Please refer to our LLM policy (https://neurips.cc/Conferences/2025/LLM) for what should or should not be described.